J. Cell. Mol. Med. Vol 15, No 4, 2011 pp. 796-808

Differentiation and migration properties of human foetal umbilical cord perivascular cells: potential for lung repair

Tiziana Montemurro [a, #], Gabriella Andriolo [a, #], Elisa Montelatici [a], Gaia Weissmann [b], Mihaela Crisan [c], Maria Rosa Colnaghi [b], Paolo Rebulla [a], Fabio Mosca [b], Bruno Péault [c, d], Lorenza Lazzari [a, *]

[a] *Cell Factory, Center of Transfusion Medicine, Cellular Therapy and Cryobiology, Department of Regenerative Medicine, Fondazione Ospedale Maggiore Policlinico, Mangiagalli e Regina Elena, Milan, Italy*
[b] *Neonatologia e Terapia Intensiva Neonatale, Fondazione Ospedale Maggiore Policlinico, Mangiagalli e Regina Elena, Università degli Studi di Milano, Milan, Italy*
[c] *Stem Cell Research Center Department of Pediatrics, Children's Hospital of Pittsburgh, Pittsburgh, PA, USA*
[d] *David Geffen School of Medicine at UCLA-Orthopaedic Hospital Research Center, Los Angeles, CA, USA*

Received: July 28, 2009; Accepted: February 23, 2010

ABSTRACT

Mesenchymal stem cells (MSC) have been derived from different cultured human tissues, including bone marrow, adipose tissue, amniotic fluid and umbilical cord blood. Only recently it was suggested that MSC descended from perivascular cells, the latter being defined as $CD146^+$ neuro-glial proteoglycan $(NG)2^+$ platelet-derived growth factor-$R\beta^+$ ALP^+ $CD34^-$ $CD45^-$ von Willebrand factor $(vWF)^-$ $CD144^-$. Herein we studied the properties of perivascular cells from a novel source, the foetal human umbilical cord (HUC) collected from pre-term newborns. By immunohistochemistry and flow cytometry we show that pre-term/foetal HUCs contain more perivascular cells than their full-term counterparts (2.5% *versus* 0.15%). Moreover, foetal HUC perivascular cells (HUCPC) express the embryonic cell markers specific embryonic antigen-4, Runx1 and Oct-4 and can be cultured over the long term. To further confirm the MSC identity of these cultured perivascular cells, we also showed their expression at different passages of antigens that typify MSC. The multilineage differentiative capacity of HUCPC into osteogenic, adipogenic and myogenic cell lineages was demonstrated in culture. In the perspective of a therapeutic application in chronic lung disease of pre-term newborns, we demonstrated the *in vitro* ability of HUCPC to migrate towards an alveolar type II cell line damaged with bleomycin, an anti-cancer agent with known pulmonary toxicity. The secretory profile exhibited by foetal HUCPC in the migration assay suggested a paracrine effect that could be exploited in various clinical conditions including lung disorders.

Keywords: lung repair • pericytes • umbilical cords • newborns

Introduction

Mesenchymal stem cells (MSC) are multipotent precursors able to differentiate into various mesodermal cell types [1]. These cells, for which a unique set of markers – that should allow their direct purification – is still missing, have been isolated retrospectively from bone marrow and several other tissues, by adherence to culture plastic.

A close resemblance between MSC and pericytes has been uncovered, suggesting a perivascular origin for the former [2–6] and suggesting why MSC can be isolated from all tissues. Pericytes, also known as mural cells or Rouget cells [7–8] are closely adherent to endothelial cells in capillaries and microvessels. Pericytes have been identified in some tissues [9–12] based on the expression of different antigens and only in a very recent work did some of us validate a set of markers to precisely localize and isolate pericytes/perivascular cells in human foetal and adult organs including muscle, pancreas, bone marrow, adipose tissue and placenta. Moreover, we demonstrated for the first time that these cells can give rise to MSC in culture, thus the elusive MSC

[#]These authors contributed equally to this work.
*Correspondence to: Lorenza LAZZARI, Ph.D.,
Cell Factory, Center of Transfusion Medicine,
Cell Therapy and Cryobiology, Department of Regenerative Medicine,
Fondazione Ospedale Maggiore Policlinico, Mangiagalli e Regina Elena,
Via F. Sforza 35, 20122 Milan, Italy.
Tel.: +39 02 5503 4053
Fax: +39 02 5503 2796
E-mail: cbbank@policlinico.mi.it

doi:10.1111/j.1582-4934.2010.01047.x

[13]. The human perivascular cell is defined by expression of NG2, a proteoglycan expressed during vascular morphogenesis [14–15], CD146 (aka S-endo1, Mel-CAM, Muc18 or gicerin), an endothelial cell antigen also expressed at the surface of pericytes [16–18] and platelet-derived growth factor (PDGF)-Rβ, a tyrosine-protein kinase implicated in the control of cell proliferation, survival and migration.

Human umbilical cord (HUC) has been mainly used as a source of endothelial cells (HUVEC) [19–20] and of mesenchymal stromal cells derived from the Wharton's jelly (WJ) [21–22].

In this study, we localized perivascular cells present in the human full-term umbilical cord and, at a higher frequency, in the foetal (pre-term) cord. We isolated, characterized and expanded these cells in culture and we show that they exhibit the features of MSC, being able to differentiate into mesodermal cell lineages and to migrate towards a damaged tissue. These properties are particularly relevant in view of cellular therapy applications in pre-term newborns, for instance those who are at high risk for chronic lung disease or bronchopulmonary dysplasia (BPD). In fact, although the survival of premature newborns has improved and refinement in neonatal intensive care has modified the outcome of BPD, attempts to prevent or treat this disease are still disappointing. This context prompted us to envision pre-term HUC perivascular cells as novel therapeutic stem cells for treating lung disorders in premature newborns.

Materials and methods

Isolation and culture of human umbilical cord perivascular cells

HUCs from pre-term (23–32 weeks of gestation; $n = 24$) and full-term ($n = 7$) newborns were obtained after informed consent from 31 pregnant women. HUC (median length 14 cm, range 8–24) were dissected longitudinally to expose the WJ, the vein and the two arteries and the ends of the cords were sutured in order not to digest the internal walls of the vessels (Fig. 1A). The samples were digested with 1 mg/ml collagenase A (Roche Diagnostics GmbH; Mannheim, Germany) at 37°C until perivascular regions were dissociated, for a maximum of 18 hrs. The non-digested material was discarded and the cell suspension was collected, diluted with phosphate-buffered saline (PBS; Gibco, Grand Island, NY, USA) to reduce the viscosity and centrifuged at 1400 rpm for 10 min. The pellet was resuspended and the HUC perivascular cells (HUCPC) were seeded in EGM2 medium (Lonza, Walkersville, MD, USA) on a pre-coated gelatine layer (Sigma-Aldrich; St. Louis, MO, USA). After 1 week, the medium was replaced with DMEM high-glucose (Invitrogen, Carlsdad, CA, USA), supplemented with 20% foetal bovine serum (FBS; Biochrom, AG, Berlin, Germany) and 1% penicillin/streptomycin (P/S, Sigma-Aldrich) and maintained in long-term culture at 37°C in a humidified atmosphere containing 5% CO_2. Adherent cells, 80% confluent, were passaged by treatment with trypsin-ethylenediaminetetraacetic acid (Gibco), and split 1:3 in uncoated plates in the same culture conditions. Medium was changed every 3 days.

Immunohistochemistry

Fresh pre- and full-term HUC were gradually frozen by immersion in isopentane (Merck Group, Frankfurter, Germany) cooled in liquid nitrogen and embedded in tissue freezing medium (Triangle Biomedical Sciences, Durham, NC, USA). Seven micrometre sections were cut on a cryostat (Thermo Scientific Microm, Walldorf, Germany) and fixed for 5 min. with 50% acetone (VWR International, West Chester, PA, USA) and 50% methanol (Fischer Scientific, Pittsburgh, PA, USA) or for 10 min. in 4% paraformaldehyde (Sigma-Aldrich). Sections were dried for 5 min. at room temperature (RT), washed three times for 5 min. in PBS and blocked with 5% goat serum (Gibco) in PBS for 1 hr at RT. Sections were incubated with uncoupled primary antibodies overnight at 4°C, or 2 hrs at RT in the case of directly coupled antibodies. After rinsing, sections were incubated for 1 hr at RT with a biotinylated secondary antibody, then with fluorochrome-coupled streptavidin, both diluted in 5% goat serum in PBS. The following uncoupled anti-human primary antibodies were used: anti-CD146 (BD, Becton Dickinson, San Jose, CA, USA; 1:100), anti-CD31 (DAKO, Glostrup, Denmark, 1:100), CD34⁻fluorescein isothiocyanate (FITC) (DAKO, 1:50) and anti-CD105 (Invitrogen, 1:50). The coupled antibodies were: biotinylated anti-CD144 (BD, 1:100), α-smooth muscle actin-FITC (SMA, Sigma-Aldrich, 1:100) and biotinylated anti-CD146 (Miltenyi Biotec, Gladbach, Germany, 1:11). Streptavidin-Cy3 (Sigma-Aldrich, 1:500) and streptavidin-Cy5 (CyDye, 1:500) were used in conjunction with biotinylated antibodies. Uncoupled *Ulex europaeus* agglutinin I (UEA-I; Vector Laboratories, Burlingame, CA, USA; 1:100) was also used. Nuclei were stained with DAPI (4′, 6-diamino-2-phenylindole dihydrochloride; Molecular Probes, Inc., Eugene, OR, USA; 1:2000) for 5 min. at RT. An isotype-matched negative control was performed with each immunostaining where the primary antibody was omitted and replaced by PBS supplemented with 5% of goat serum. Slides were mounted in glycerol-PBS (1:1, Sigma-Aldrich) and observed on an epifluorescence microscope (Nikon Eclipse TE 2000-U, Nikon Corporation, Tokyo, Japan). Alternatively, sections were analysed on an Olympus Fluoview 1000 confocal microscope equipped with 100× oil immersion optics.

RNA isolation and RT-PCR analysis

Total RNA was extracted from 3×10^5 to 1×10^6 foetal HUCPC using the RNeasy Mini Kit (Qiagen AG, Hilden, Germany). The total RNA was eluted in a final volume of 40 μl, and its quality, integrity and size distribution was assessed by optic density (absorbance at 260/280 nm and ratio of >1.8). Four ng of cDNA were used for each PCR assay. The primers used for PCR are listed in Table 1. Positive controls were obtained from the corresponding foetal tissues.

Glyceraldehyde 3-phosphate dehydrogenase (GAPDH) was used as a housekeeping gene. The primers were constructed on the basis of published human sequences, and selected using version 1.5 of the Primer Express software available from Applied Biosystems (Applied Biosystems, Inc., Foster City, CA, USA). Each set of oligonucleotides was designed to span two different exons. The samples were loaded on 1% agarose gels.

Flow cytometry analysis

HUCPC isolated from foetal and term cords were characterized by flow cytometry before and during culture. Cells were washed in PBS for 20 min. at RT and incubated in the dark with the following directly coupled mouse anti-human antibodies: CD13-phycoecythrin (PE) (BD), CD34-PE (BD), CD44-FITC (BD), CD45-PC7 (Beckman Coulter, Fullerton, CA, USA), CD56-PE

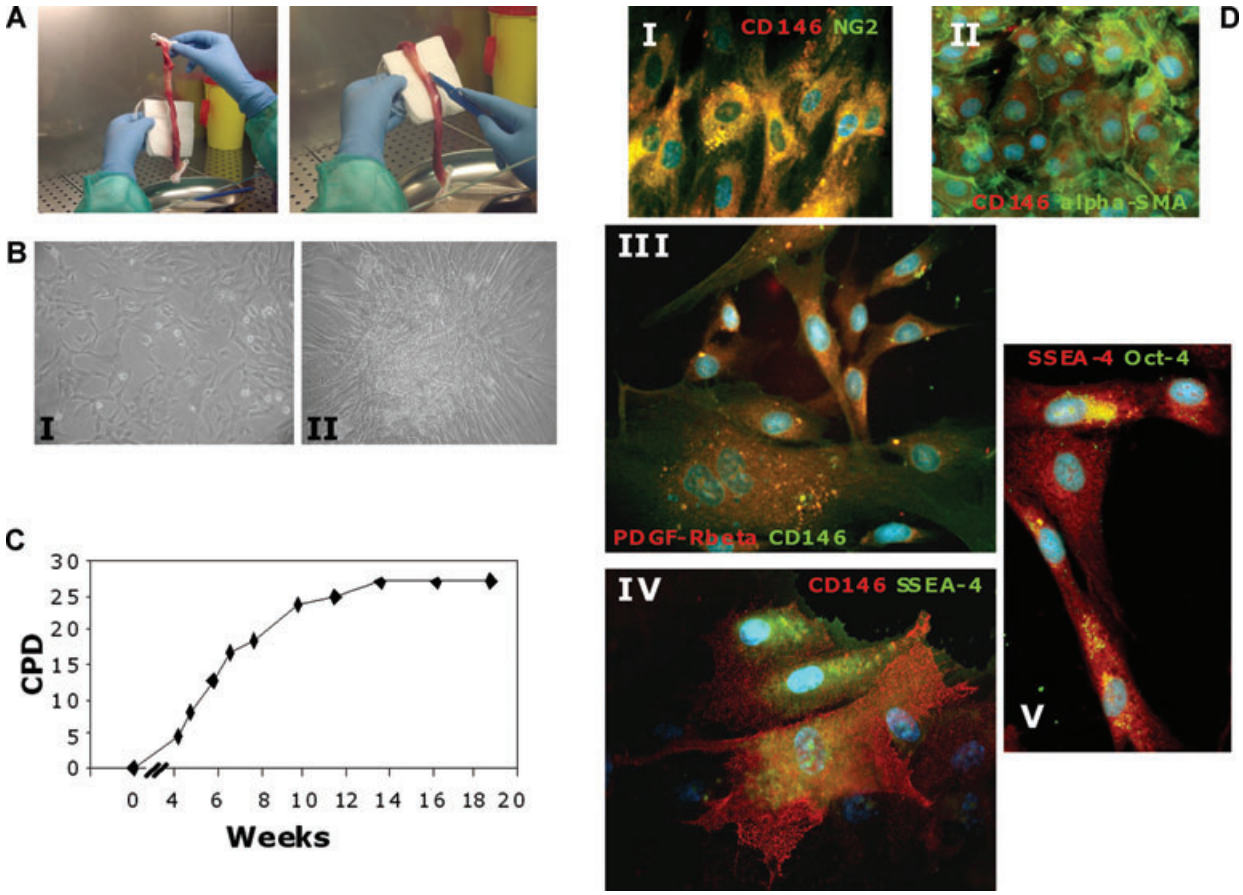

Fig. 1 Isolation, culture and immunocytochemical characterization of HUCPC. The dissection under sterile condition of foetal and full-term cords was performed to expose the WJ, the vein and arteries (**A**). After the *in vitro* expansion of foetal HUCPC (**B**) the cells showed a homogeneous morphology (B I, 20×) and form 'round bottom' colonies (B II, 40×). (**C**) The growth rate of foetal HUCPC, calculated as cumulative number of population doublings (CPD), was fastest during weeks 4–10 of expansion. (**D**) The immunocytochemistry analysis at passage 3 of the culture showed that foetal HUCPC are positive for CD146 (I, II, IV: red; III: green) and co-expressed NG2 (I: green), α-SMA (II: green), PDGF-Rβ (III: red) and SSEA-4 (IV: green). Moreover, the SSEA-4$^+$ cells (V: red) expressed also Oct-4 (V: green). All the cells (I–V) were stained with DAPI (blue). Magnification: I–II 40×; III–V 60×. All the slides were analysed using a Video Confocal Microscope (ViCo-Eclipse 80i, Nikon) equipped with a Plan Fluor 40× 1.30 DIC H/N2 Oil objective or with a Plan Apo VC 60×/1.40 oil DIC N2 (Nikon).

(Chemicon, Temecula, CA, USA), CD73-PE (BD), CD90-PE (Chemicon), CD105-PE (ImmunoTools, Friesoythe, Germany), CD133-PE (Miltenyi Biotec), CD146-PE/FITC (BioCytex, Marseille, France), α-SMA FITC (Sigma-Aldrich), NG2-PE (Beckman Coulter), PDGF-Rβ PE (BD), human leukocyte antigen (HLA)-ABC-FITC (BD), HLA-DR (BD), CD144-FITC (VE-cadherin; Bender MedSystem, Burlingame, CA, USA). The isotype-matched immunoglobulins IgG1 PE-FITC (Chemicon), IgG1-PC7 (Beckman Coulter) and IgG1-APC (BD) were used as negative controls under the same conditions. After staining the cells were washed once with PBS containing 0.1% bovine serum albumin. At least 50,000 events were acquired with a Cytomics FC500 flow cytometer (Beckman Coulter) and plots were generated using the CXP analysis software.

Immunocytochemistry

Foetal HUCPC were first fixed with cold methanol/acetone (1:1) for 2 min. When necessary, cells were permeabilized with 0.1% Triton X-100 (10 min.), then washed in PBS (Gibco). Non-specific binding sites were blocked with PBS containing 2% bovine serum albumin (Sigma-Aldrich) for 20 min. at RT. Cells were incubated with directly coupled anti-human antibodies: CD146-FITC/PE (ByoCytex, Marseille, France; 1:20), NG2-PE (Immunotech, Marseille, France; 1:50), CD34-FITC (DAKO, 1:50), CD144-FITC (Bender MedSystems, 1:25), α-SMA-FITC (Sigma-Aldrich, 1:100), PDGF-Rβ PE (BD, 1:20) for 1 hr at RT. Uncoupled mouse anti-human antibodies were: CD133 (Miltenyi, Miltenyi Biotec; 1:50), vWF (DAKO; 1:40), stage-specific embryonic antigen-4 (SSEA-4; Chemicon, 1:25), pro-surfactant protein C (Chemicon, 1:100) and rabbit polyclonal antibody anti-human Oct-4 (Chemicon, 1:50). Uncoupled UEA- I (Vector, 1:100) was also used. After staining with primary unconjugated antibodies, cells were incubated with FITC-conjugated goat antimouse antibody (Exalpha Biolologicals Inc., Shirley, MA, USA. 1:300), with PE-conjugated goat anti-mouse antibody (Exalpha, 1:300), or with FITC-conjugated goat anti-rabbit antibody (Vector, 1:300) for 1 hr at RT. Nuclear counterstaining with DAPI (Roche Diagnostic Corporation, Indianapolis, IN, USA) was performed for

Table 1 Sequences of human-specific primers used for PCR analysis of foetal HUCPC

Primers		
CD45	F -catgtactgctcctgataagac	R- gcctacacttgacatgcatac
CD146	F -aaggcaacctcagccatgtcg	R- ctcgactccacagtctgggac
CD34	F -catcactggctatttcctgatg	R- agccgaatgtgtaaaggacag
CD31	F -gaagtacggatctatgattcag	R- gtgagtcacttgaatggtgca
MyoD	F -cagcgaatgcagctctcaca	R- agttgggcatggtttcatctg
Myf5	F -cagtcctgtctggtccagaa	R- ggaactagaagcccctggag
Pro-surfactant protein C	F -tgaaacgccttcttatcgtgg	R- cctgcagag age att ccatct
Oct-4	F -acatgtgtaagctgcggcc	R- gttgtgcatagtcgclgcttg
Runx1	F -tcaclgtgatggctggcaat	R- ctgcatctgactctgaggctga
Rex1	F -aaacatgagccagcaactgaag	R- agaaatcatcccctccgagag
Sox-2	F -accagaaaaacagcccgga	R- tcatgagcgtctlggttttcc
CD144	F -tctctgtttgttgaggaccc	R -aagtggtagaaaggctgctg
GAPDH	F -gcttgtcatcaatggaaatccc	R- tccacacccatgacgaacatg

15 min. at RT. An isotype-matched negative control was performed with each immunostaining where the primary antibody was omitted and replaced by PBS supplemented with 2% of FBS. All slides were mounted with DakoCytomation Fluorescent Mounting Medium (DakoCytomation, Glostrup, Denmark) and the cells were analysed using a video confocal microscope (ViCo-Eclipse 80i, Nikon, Tokyo, Japan) equipped with Plan Fluor 40× 1.30 DIC H/N2 and Plan Apo VC 60×/1.40 DIC N2 oil objectives (Nikon). Photographs were acquired with a CCD cooled interline-transfer FireWire camera (Nikon) and processed using Media Cybernetics Image Pro Plus (Media Cybernetics Inc., Bethesda, MD USA).

Pictures of the migration assay were taken with a Plan Fluor (Nikon) 100×/1.30 oil numeric aperture objective and a DS camera control (DS-5M, Nikon). Images were captured using a Nikon Digital Slide DS-L1 (Nikon), merged and analysed with Adobe Photoshop 5.5 software (Microsoft Corporation, Washington, DC, USA).

Cell lineage differentiation

Foetal HUCPC at passage 3 were differentiated into adipogenic, osteogenic and myogenic cell lineages in different media. To promote adipogenic differentiation, HUCPC were plated at 2.1×10^4 cells/cm^2 in human MSC Adipogenic Induction (catalogue number PT-3102B/PT-4135) and Maintenance (catalogue number PT-3102A/PT-4122) Medium (Lonza). At confluence, three cycles of induction/maintenance were performed, then HUCPC were cultured for seven more days in supplemented adipogenic differentiation maintenance medium (Lonza), replacing the medium every 2–3 days. The cells were stained with Oil Red O solution (Sigma-Aldrich) to detect lipid vacuoles. For osteogenic differentiation, 3.1×10^3 cells/cm^2 were grown for 3 weeks in human MSC osteogenic medium (catalogue number PT-3924/PT4120 Lonza). Induced cells were first fixed with 70% ethylic alcohol for 1 hr and then stained with Alizarin Red S 40 mM (Sigma-Aldrich) for 10 min. to detect the presence of calcium deposits.

Images of colorimetric assays were acquired on a Nikon Eclipse TS100 microscope equipped with 40×/0.55 Ph1 ADL and 20×/0.40 Ph1 ADL objectives and photographs were taken with a Nikon Digital Slide DS-L1.

For muscle differentiation, a mouse skeletal muscle cell line (G-7 line) was purchased from ATCC (CRL-1447, Manassas, VA, USA) and was used for the co-culture experiments to promote myotube formation.

First, the G-7 cells were seeded on a cover glass in a defined medium including DMEM low glucose, 20% FBS (Biochrom), 10% horse serum (Biodesigned International, Saco, ME, USA), 0.5% chick embryo extract (US Biological, Swampscott, MA, USA) and 1% P/S (Sigma-Aldrich). After 12 hrs, a defined medium containing 5-azacytidine (3 μM) was added and replaced 24 hrs later with a 5-azacytidine-free defined medium. Afterwards, 50×10^3 foetal HUCPC were first stained with the fluorescent dye PKH26, using PKH26 Red Fluorescent Cell Linker Kit (Sigma-Aldrich) following manufacturer's instructions and then co-cultured for at least 21 days with the G-7 cells. A parallel co-culture was performed with a non-damaged G-7 cell line under the same culture conditions as control.

For muscle differentiation the expression of specific myogenic markers such as spectrin (Novocastra, Newcastle, UK) and dystrofin (Novocastra) was analysed by immunocytochemistry. The antibodies strongly reacted with the domain of human spectrin and dystrophin, while no reactivity with mouse tissue was observed. All slides were analysed on a video confocal microscope. For all the differentiation cultures negative controls were set up replacing the specific lineage induction media with the standard expansion media.

Migration assay

The alveolar type II epithelial rat cell line (ATII) (CRL-2300, ATCC) was cultured in Ham's F12 medium (Invitrogen), 10 μg/ml bovine pituitary extract (Gibco), 2.5 ng/ml insulin-like growth factor-I (PeproTech EC Ltd., London, England), 2.5 ng/ml epidermal growth factor (PeproTech), 10% FBS (Biochrom) and insulin-transferrin-selenium (Gibco).

For the migration assay, 1.5×10^4/cm^2 ATII cells were first grown on a pre-coated glass slide (0.01% poly-L-lysine for 30 min., Sigma-Aldrich) in a humidified atmosphere at 37°C 5% CO_2 (Fig. 6B, I). The culture medium was replaced once until 80% cell confluence was reached. Different concentrations of bleomycin (5–50 μg/ml) (Aventis, Paris,

France) and times of exposure (12–72 hrs) were tested on ATII cells to optimize a subletal damage (data not shown). The concentration of 10 μg/ml bleomycin was eventually chosen. The ATII cell line was damaged for 40 hrs, and then the medium was replaced. 24 hrs after damage, foetal HUCPC were first stained with the fluorescent dye PKH26, a Red Fluorescent Cell Linker Kit (Sigma-Aldrich) following manufacturer's instructions, then co-cultured (5×10^4 cells/well) in transwells (8.0 μm pore size) with the damaged cell line. A parallel co-culture was performed under the same conditions with non-damaged ATII cells as a control. Migration of the PKH26$^+$ cells was evaluated every day with the inverted fluorescence microscope. After 14 days, the samples were fixed with cold methanol/acetone (1:1) for 2 min. and migratory HUCPC in contact with the damaged alveolar cell layer were stained for pro-surfactant protein C (Chemicon, 1:100), CD146 (BioCytex, 1:20), anti-α SMA FITC (Sigma-Aldrich, 1:100) and then with FITC-conjugated goat anti-rabbit antibody (Exalpha, 1:300). In addition to exclude the possibility that migratory activity of HUCPC was caused by different ATII cell density, several cell concentrations (from 5×10^3 to 20×10^3) of undamaged ATII were tested as an additional control and co-cultured with PKH26$^+$ HUCPC.

Chemotaxis assay

Chemotactic responses were measured by a modified Boyden chamber assay, using a 24-well chamber with polycarbonate filters (8.0 μm pore size) coated with Matrigel basement membrane matrix (BioCoat Invasion Assay, BD). The lower wells were filled with conditioned medium collected from damaged ATII cells and covered by the chemotaxis filter. The HUCPC ($n = 4$) were trypsinized, counted, and the upper wells were filled with 5×10^4 HUCPC in DMEM. After 24 hrs incubation, the filter was carefully removed and non-migrated cells on the upper side eliminated by rinsing with cold PBS and scraping over a rubber wiper. The migrated cells on the lower side of the filter were fixed with cold acetone/methanol 1:1 (v:v) for 3 min. and stained with DAPI. In the controls, the lower wells were filled with medium collected from undamaged ATII cells. HUCPC that migrated through the filter pores and attached underneath the membrane were counted by microscopy. The number of migrated cells in control and stimulated wells was counted at 100× magnification. Results were expressed as chemotactic index, determined as the average number of migrated cells in stimulated wells divided by average number of migrated cells in control wells.

ELISA

A quantitative sandwich enzyme immunoassay technique (Quantikine, R&D Systems, Minneapolis, MN, USA) was used following the manufacturer's instructions to evaluate the production of soluble factors by HUCPC.

During the co-culture of foetal PKH26$^+$ HUCPC with damaged ATII epithelial cells, supernatants from six independent experiments were collected at different times (24, 48, 72 hrs after damage) and immediately stored at –20°C until evaluation. As controls, supernatants were collected from (1) a co-culture of PKH26$^+$ HUCPC with non-damaged ATII cells; (2) damaged ATII cultured cells; (3) cultured HUCPC. The evaluated soluble factors were: keratinocyte growth factor (KGF), PDGF-BB and vascular endothelial growth factor (VEGF). The optical density of each sample was determined using a microplate reader set to 450 nm (Genios Plus, TECAN, Salzburg, Austria). Data were analysed using Magellan Software and expressed as mean picograms of the secreted factors per millilitre at the time of harvest.

Statistical analysis

The Wilcoxon-based method was used to determine the significance of differences between independent groups. Statistical significance level was defined as $P < 0.05$.

Results

(1) Immunohistochemical detection of perivascular cells in foetal and term umbilical cords

Immunohistochemistry was used to detect the presence of perivascular cells in different umbilical cord compartments including WJ, vein and arteries. To this end, we examined two foetal and three term cords. Perivascular smooth muscle cells surrounding the big vessels present in the foetal cord co-express CD146 and SMA. Only in the foetal cord we could also detect microvessels, arteriole and veinule, with diameters ranging from 10 to 100 μm (Fig. 2A). Perivascular cells presented the same phenotype in small and big vessels and they did not express the known endothelial cell markers CD144, CD34, CD31, UEA-1 receptor.

The distribution of CD146 and α-SMA in umbilical cords at term was slightly different. First, no small blood vessels were found in term cords. The 2 arteries present numerous perivascular cell layers, all co-expressing CD146 and α-SMA. The vein had a particular phenotype since only rare CD146high α-SMA+ cells were observed within the vascular wall, especially at the distal periphery (Fig. 2C). All other venous perivascular cells strongly expressed α-SMA but not CD146.

In both foetal and term WJ, no cells expressing CD146, CD144, CD34, CD31 or the UEA-1 receptor were found. WJ cells express CD105 (Fig. 2B and D) and α-SMA (not shown). The frequency of these CD105$^+$ cells was much lower in term cords than in the foetal counterpart cords.

(2) Morphology, phenotype and molecular profile of HUCPC

The digestion procedure yielded an average of 1–8.2×10^6 cells per HUC depending on the length of HUC harvested, which ranged from 8 to 24 cm. Foetal and term HUC were then processed before culture to characterize perivascular cells by flow cytometry. CD56$^+$ cells, as well as hematopoietic cells (CD45$^+$) were initially gated out [23]. Perivascular cells were identified by high CD146 expression and lack of CD34, the latter to ascertain the absence of endothelial cells. Interestingly, the perivascular cell population (CD146$^+$ CD34$^-$ CD45$^-$ CD56$^-$) was observed mainly in foetal samples, rather than in term cords (2.5% *versus* 0.15%), confirming immunohistochemistry observations. These cells clearly expressed PDGF-Rβ. All of the results of immunocytochemistry are reported in Table 2.

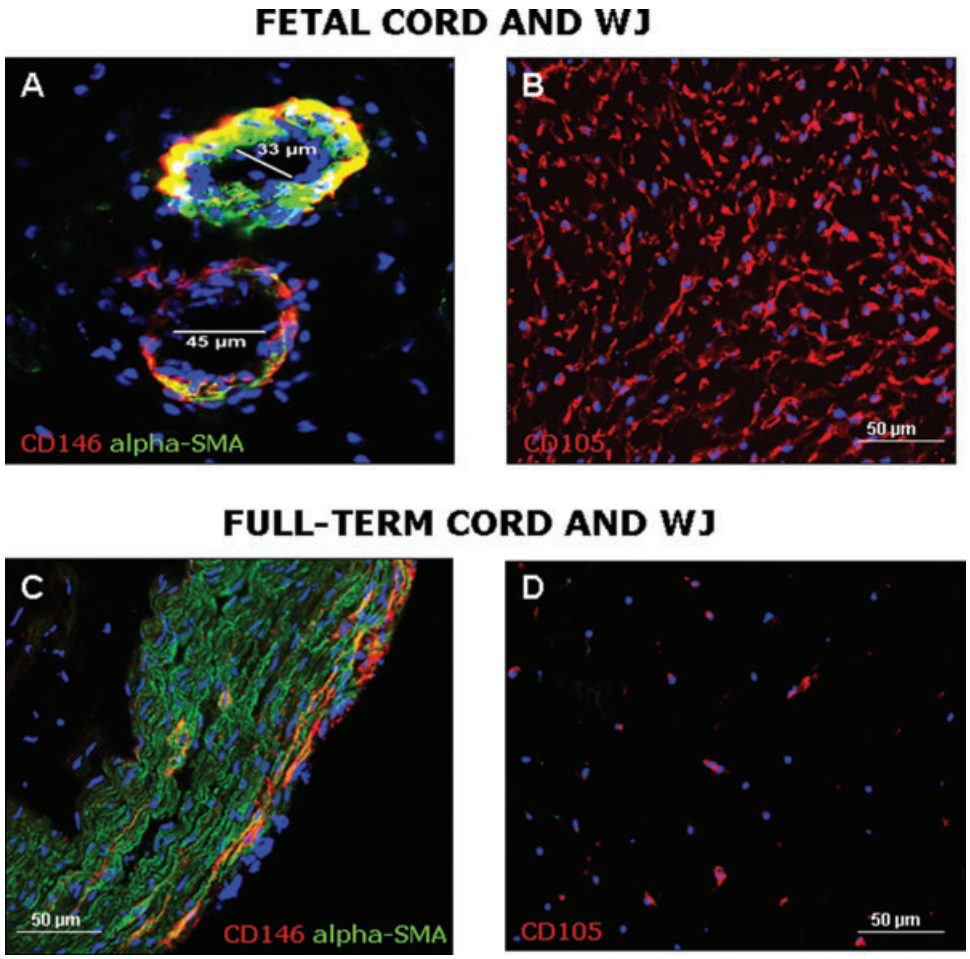

Fig. 2 Localization of HUCPC in sections of foetal and full-term HUC by immunohistochemistry. The presence of HUCPC co-expressing CD146 (red) and α-SMA (green) was also detected around microvessels of foetal HUC (**A**; magnification 400×). Cells co-expressing CD146 and α-SMA were identified with a low frequency in the peripheral vascular wall of full-term HUC (**C**; magnification 200×). WJ cells expressing CD105 (red) were much lower in full-term cords (**D**; magnification 200×) than in the foetal cords sections (**B**; magnification 200×).

Further experimental strategy was focused on foetal cord cell isolation, since it is richer in perivascular cells. Our cell isolation approach consisted of a strategy including the ligation of the ends of cords and appropriate culture conditions that led us to exclude as much as possible the endothelial contamination from the beginning and to selectively favour the growth of the perivascular cells.

These cells, maintained in long-term culture, exhibited a spindle shape (Fig. 1B, I) and formed 'round bottom' colonies (Fig. 1B, II). The growth rate was calculated as cumulative number of population doublings during weeks [24]. Growth was slow in the first 3 weeks and the fastest rate was during weeks 4–10 (Fig. 1C).

At passage 3, cultured cells were detached by trypsin and characterized by flow cytometry. Foetal HUCPC were positive for CD90 (median 100%, range 97–100), CD73 (84%, 74–93), CD105 (86%, 30–100), CD44 (90%, 80–99) and HLA-ABC (97%, 60–100). They also expressed CD146 (63%, 23–81), NG2 (19%, 9–25), PDGF-Rβ, (93%, 85–95), α-SMA (60%, 40–80), but not CD34, CD45 and CD56. Moreover, foetal HUCPC were negative for CD133, CD144 and HLA-DR expression, confirming their MSC-like profile (Fig. 3). Comparable percentages were found at passage 6.

Table 2 Comparison of the expression of surface markers in foetal - and full-term HUCPC after the isolation and before the cell expansion (human foetal umbilical cords $n = 24$, human term umbilical cords $n = 7$). The results are expressed as mean ± S.D.

Cell markers	Foetal cord (%)	Term cord (%)
$CD146^+$ $CD34^-CD45^-$ $CD56^-$	7.44 (13.94)	0.93 (1.70)
$CD146^+$ $PDGF\text{-}R\beta^+$	11.58 (6.12)	0.33 (0.40)
$\alpha-SMA^+$ $NG2^+$	0.34 (0.39)	0.67 (1.49)
$\alpha-SMA^+$	56.20 (24.49)	53.72 (40.11)
$NG2^+$	17.88 (27.50)	13.94 (22.42)
$CD144^+$	11.13 (11.31)	6.26 (5.88)
$PDGF^-R\beta^+$	12.92 (14.59)	3.93 (6.38)

As illustrated by Figure 1D (I), $CD146^+$ cultured perivascular cells were also positive for NG2, α-SMA (Fig. 1D, II) and PDGF-Rβ (Fig. 1D, III) expression. In contrast, perivascular cells did not express endothelial cell markers such as CD144, CD34, CD133

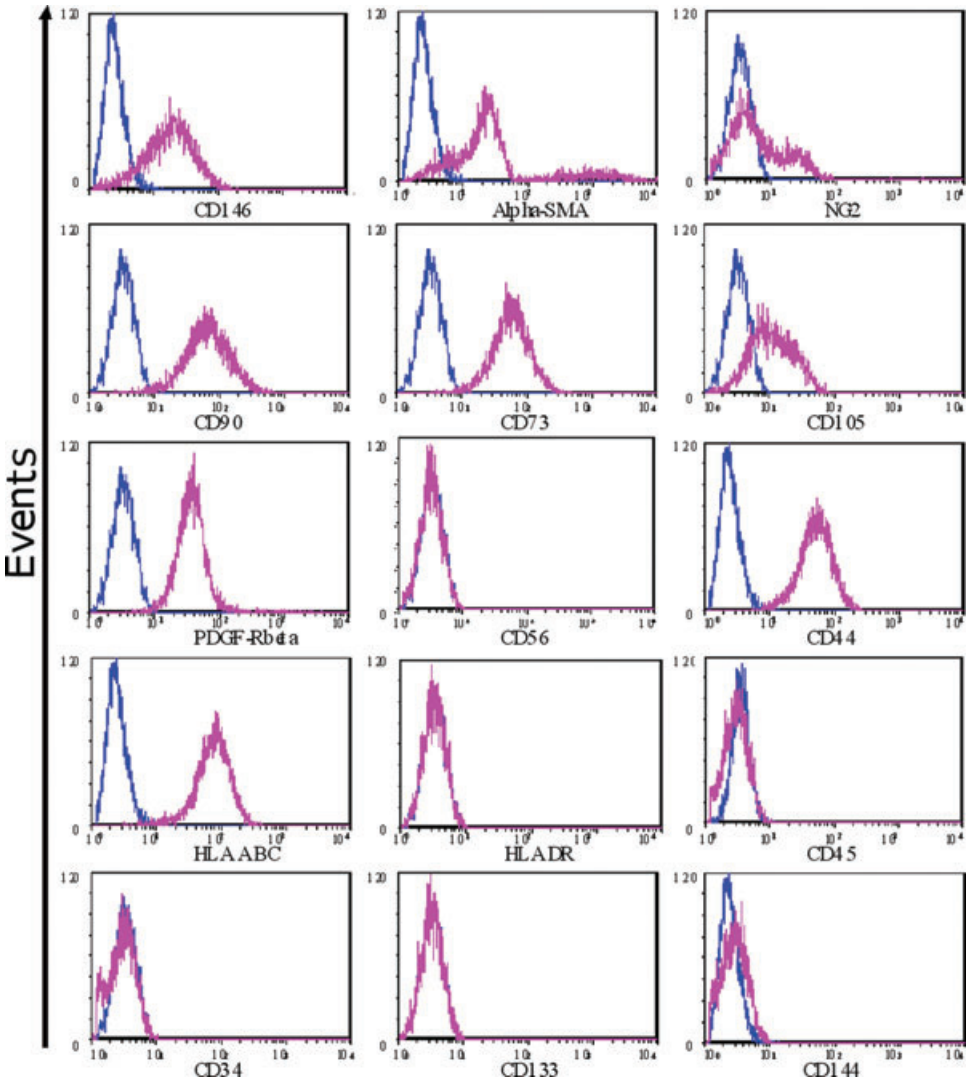

Fig. 3 Representative flow cytometry analysis of expanded foetal HUCPC. After three passages of culture the cells ($n = 24$) were detached with trypsin, washed and stained with directly labelled monoclonal antibodies (pink histograms) or exposed to isotype-matched non-immune directly labelled immunoglobulins (blue histograms). Foetal HUCPC were positive for CD146, PDGF-Rβ, α-SMA and NG2, while were negative for CD45, CD34 and CD56 confirming the main features of perivascular cells. Moreover they expressed the typical mesenchymal markers such as CD90, CD73, CD105, CD44, HLA-ABC and they were negative for CD133, CD144 and HLA-DR.

and the UEA-I receptor (Table 3). Moreover, HUCPC co-expressed the embryonic stem cell markers SSEA-4 and a relatively low level of Oct-4 (Fig. 1D, IV–V).

Cultured perivascular cells were also analysed by RT-PCR for the expression of embryonic, myogenic and endothelial cell markers, showing that foetal HUCPC express Runx1 and Oct-4 at different levels, which characterize the undifferentiated stem cell state, and CD146, while they are negative for Rex1, Sox2, Myo-D, Myf5, CD31, CD45, CD34 and CD144, thus excluding any myogenic and endothelial cell contamination (Fig. 4).

(3) Differentiation potential

To further explore a possible affiliation between MSC and cultured umbilical cord perivascular cells, HUCPC were cultured under appropriate inductive conditions promoting their differentiation into osteogenic, adipogenic and myogenic cell lineages.

Table 3 Immunocytochemical analysis of cultured foetal HUCPC. Results are expressed as positive (+) or negative (−) cells on the total number of counted cells.

Cell markers	Foetal cord
CD146	+
PDGF-Rβ	+
α-SMA	+
NG2	+
CD34	−
CD133	−
CD144	−
UEA-I	−
Oct-4	+
Pro-surfactant protein C	−

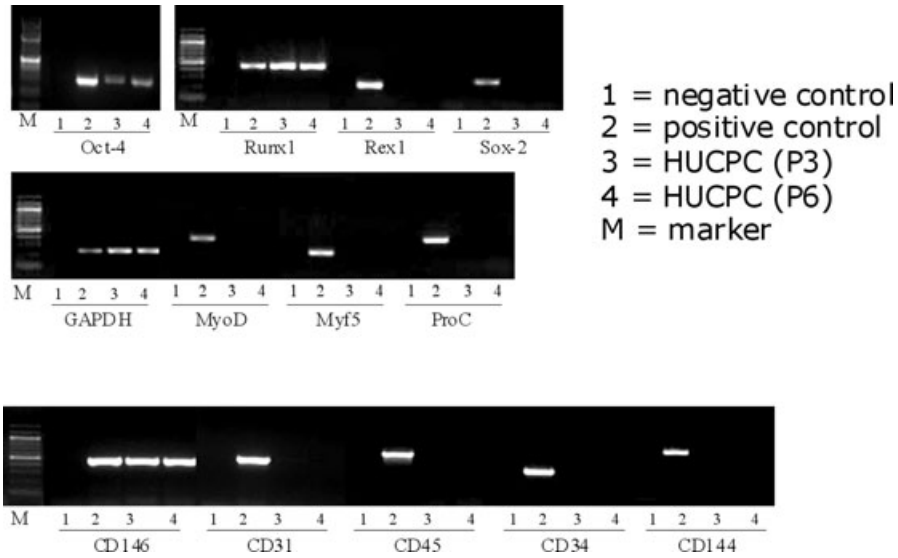

Fig. 4 RT-PCR expression profile of foetal HUCPC. RT-PCR was perfumed with total RNA extracted from expanded foetal HUCPC and the cDNA obtained was used for PCR assays to evaluate the expression of embryonic, myogenic, endothelial and hematopoietic markers. Negative controls (lane 1) were performed with the reaction mix without the cDNA. Positive controls (lane 2) were obtained from the corresponding foetal tissues. The samples of foetal HUCPC used were at different passage of culture (lane 3: passage 3; lane 4: passage 6). Cultured foetal HUCPC were positive for the embryonic markers Runx1 and Oct-4, and for CD146. They were negative for the expression of other embryonic markers (Rex1, Sox-2), myogenic markers (MyoD, Myf5), endothelial markers (CD31, CD34, CD144) and hematopoietic markers (CD45, CD34).

In osteogenic conditions, HUCPC became mineralized as indicated by staining with the calcium-specific dye Alizarin red (Fig. 5A, I). Under adipogenic induction, HUCPC generated lipid vacuoles and became stainable by the triglyceride-specific dye Oil Red O (Fig. 5B, I). Perivascular cells cultured in myogenic conditions developed into typical myotubes that co-expressed the tracking marker PKH26, human dystrophin (Fig. 5C, I) and human spectrin (Fig. 5C, II). To strengthen these results, all the differentiation cultures were stained also with the non-lineage specific markers showing the absence of any other non-specific lineage commitment.

(4) Migratory ability and proteome assay

A model of tissue damage was developed using bleomycin, an antibiotic glycopeptide often used as an anti-cancer agent [25–27] (Fig. 6A). A rat alveolar cell line (Fig. 6B, I) was used to study morphological changes induced by bleomycin (5, 10, 20 or 50 μg/ml) at different time-points. The same area of each monolayer was examined under the phase-contrast microscope at time intervals of 10, 24, 40 and 72 hrs. After a 40-hr treatment with bleomycin at a concentration of 10 μg/ml, alveolar cells looked contracted and started to lose contact with their neighbours (Fig. 6B, II). At a concentration of 5 μg/ml, bleomycin did not induce significant morphological changes, while at the highest concentration of bleomycin (50 μg/ml) all cells were detached (data not shown).

Using this model of lung tissue damage, the migratory ability of HUCPC was tested. After 14 days of culture, foetal PKH26$^+$ HUCPC migrated towards the damaged alveolar cell layer (Fig. 6B, III–IV) while no migration was observed in control cultures. Moreover, additional controls showed that the undamaged ATII cells did not promote migration of PKH26$^+$ HUCPC cells even at the similar low density of the damaged ATII cells. For determining whether soluble factors released from damaged ATII cells could initiate HUCPC migration, a modified Boyden chamber assay was used testing the chemotactic activity of damaged *versus* undamaged ATII conditioned media. The mean (±S.D.) of chemotactic index, resulting from four independent experiments in duplicate, was 6.86 (±1.46).

To test the capacity of HUCPC to integrate into the damaged cell layer, secretion of the pro-surfactant protein C (Pro-C), a marker of alveolar type II pneumocytes, was tested. Four distinct proteins isolated from pulmonary surfactant are termed surfactant proteins A, B, C and D, where the C protein is the mature form. HUCPC did not express Pro-C both at the RNA (Fig. 4) and protein levels before co-culture (Fig. 6A, I). Conversely, migratory HUCPC co-expressed PKH26 and Pro-C, as assessed by immunocytochemistry (Fig. 6B, V–VI). Moreover, these cells co-expressed PKH26 together with CD146 and NG2 (Fig. 6B, VII–VIII).

At different co-culture times, supernatants were collected to determine whether angiogenic factors were also secreted. HUCPC in the presence of damage produced high levels of KGF and slight modifications of VEGF levels during the whole culture (Fig. 7) in comparison with the co-cultures with no damage. No PDGF-BB was secreted.

Discussion

Perivascular cells have been recently identified in several human tissues showing their stem cell properties. Schwab *et al.* [9]

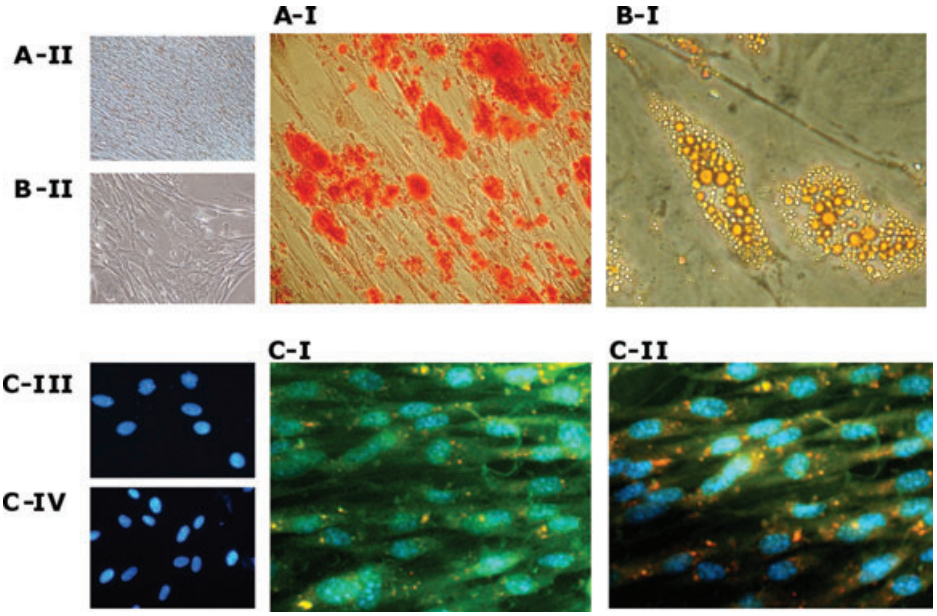

Fig. 5 (**A**) I: Alizarin red staining showing area of mineralization on HUCPC cultured in osteogenic differentiating medium (magnification 20×). (**A**) II: negative control. Slides were acquired with Nikon Eclipse TS100 equipped with a 20×/040 Ph1 ADL. (**B**) I: Oil Red O staining showing the accumulation of lipid vacuoles in HUCPC after adipogenic treatment (magnification 40×). (**B**) II: negative control. Slides were acquired with Nikon Eclipse TS100 equipped with a 40×/0.55 Ph1 ADL. (**C**) Muscle differentiation after 21 days showed the typical myotubes containing three to five nuclei and co-expressing the tracking marker PKH26 (red) and the human dystrophin (I) (green) and spectrin (II) (green) (magnification 40×). (**C**) III and IV: negative controls. Slides were analysed using a Video Confocal Microscope (ViCo-Eclipse 80i, Nikon).

showed that human endometrium contains a small population of perivascular cells that co-express CD146 and PDGF-Rβ. Dellavalle *et al.* [10] demonstrated that pericytes sorted from human skeletal muscle by alkaline phosphatase expression can regenerate skeletal myofibres in dystrophic immunodeficient mice. Even more recently, Zanettino *et al.* [11] described a multipotent perivascular cell population within adult human adipose tissue on the expression of stromal precursor antigen (STRO)-1 and 3G5. Extending these previous observations, some of us validated the $CD146^+$ $NG2^+$ PDGF-$R\beta^+$ ALP^+ $CD34^-$ $CD45^-$ vWF^- $CD144^-$ phenotype as an indicator of pericyte/perivascular cell identity throughout human foetal and adult organs including muscle, pancreas, bone marrow, adipose tissue and placenta [13]. Only Sarugaser *et al.* focused their attention on the umbilical cord as a source of perivascular cells, starting from full-term cord donors [12, 28].

Using as a marker the immunophenotype we recently validated [13] to identify human perivascular cells, we set up to further identify these cells within HUC and compare the frequency of these cells within pre- and full-term cords. We confirmed the presence of perivascular cells around the large arteries and vein in full-term cords, as already described by Sarugaser *et al.* [12]. Immunohistochemistry and, then, flow cytometry also showed that, interestingly, small vessels typically surrounded by pericytes are only present in foetal cords. The umbilical cord is formed by the fusion of yolk sac derivatives and connecting stalk mesenchyme, and by weeks 12–14 contains tightly spiralled small blood vessels. The higher frequency of pericyte-like cells we found in pre-term cords is probably related to the transient presence of these small vessels, which have disappeared at the end of gestation when the cord contains only two arteries and one vein [29]. These observations prompted us to isolate perivascular cells from foetal cords, characterize these and document their multilineage mesodermal potential. With a view to future therapeutic settings, we also tested the ability of these cells to migrate towards an injured tissue.

Since the umbilical cord is a well-known source of endothelial cells [19, 20], we first developed a combined strategy of cell isolation and cell culture to separate the perivascular cells. We excluded any endothelial cell contamination: isolated perivascular cells did not express any of the endothelial cell markers tested including CD31, CD34 and CD144 by RT-PCR (Fig. 4), CD34, CD133 and CD144 by flow cytometry (Fig. 3) and CD34, CD144, CD133, vWF and *Ulex europaeus* receptor by immunofluorescence (Table 3).

Moreover, the isolated perivascular cells were confirmed by RT-PCR and flow cytometry not to include detectable hematopoietic cells (CD34, CD45) or myogenic-like cells (CD56, MyoD, Myf5) (Figs 3 and 4). The latter could have been brought from the WJ since this gelatinous connective tissue contains cells with ultrastructural characteristics of both fibroblasts and smooth muscle cells [30]. In this regard, immunohistochemistry analysis performed on foetal and full-term cords confirmed the presence of genuine mesenchymal stromal cells in this region (Fig. 2B and D).

Moreover, HUCPC expressed SSEA-4, an early embryonic glycolipid antigen that is commonly used as a marker of human embryonic stem cells and embryos at cleavage to blastocyst stages, and which has been recently identified in the bone marrow MSC population (Fig. 1D, IV) [31, 32]. SSEA-4 was co-expressed with Oct-4, an embryonic cell marker arguably considered as an indicator of stemness (Fig. 1D, V) [33, 34]. Interestingly, HUCPC

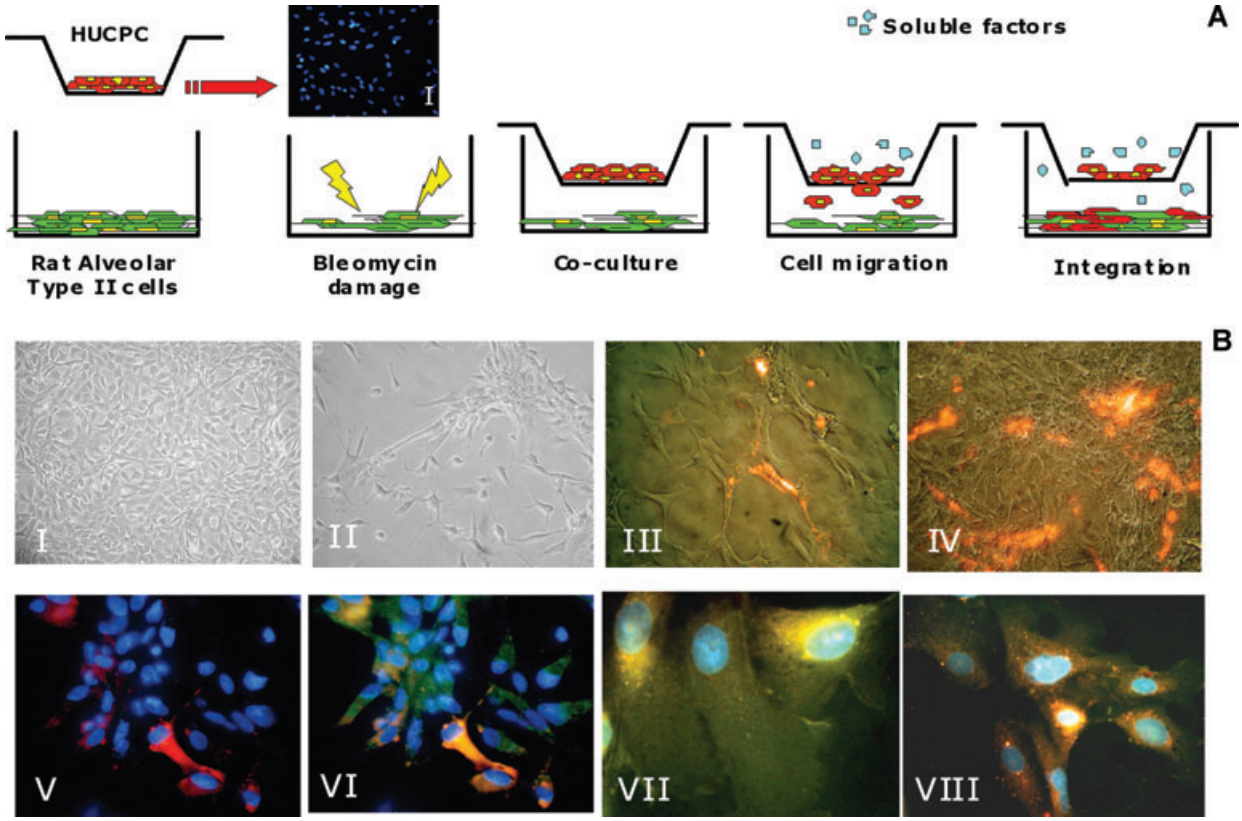

Fig. 6 Foetal HUCPC migration assay. (**A**) Rat ATII cells, grown to 80% cell confluence in multiwell, were damaged exposing to bleomycin for 40 hrs. After 24 hrs foetal HUCPC, negative for the pro-surfactant protein C (I) and stained with the red fluorescent dye PKH26, were co-cultured in transwells in the presence of the damaged cell line. During 14 days of co-culture, foetal HUCPC migrate towards the rat ATII layer. Negative control was performed with a non-damaged rat ATII cell line under the same culture conditions. (**B**) The migration was continuously evaluated with inverted fluorescence microscope to observe the rat ATII cell line before the damage with bleomycin (I), after the damage (II), during the $PKH26^+$ foetal HUCPC migration (III: red) and integration (IV: red). The migrated $PKH26^+$ foetal HUCPC (V: red) co-expressed the epithelial alveolar marker pro-surfactant protein C (VI: green). Moreover, these cells maintain the expression of the perivascular markers CD146 (VII: green) and NG2 (VIII: green). All the cells (V–VIII) were stained with DAPI (blue).

co-expressed these embryonic cell markers together with perivascular cell markers (Fig. 1D, IV) possibly as another indication of the multipotency of pericytes.

Recently, some of us demonstrated that human perivascular cells sorted from diverse human tissues and cultured over the long term give rise to adherent, multi-lineage progenitor cells that exhibit the features of MSC and concluded that pericytes are the origin of that elusive stem cell population [13]. In the present study, we also showed the expression of antigens that typify MSC on cultured HUCPC at different passages (Fig. 3). To further document a possible affiliation between HUCPC and MSC, we confirmed that cultured perivascular cells in appropriate inductive conditions differentiate towards osteogenic (Fig. 5A, I), adipogenic (Fig. 5B, I) and myogenic cell lineages (Fig. 5C, I and II).

Amongst all the stem cell populations isolated from different tissues and with multipotency characteristics, HUCPC can be particularly appealing for therapeutic approaches because they pose no ethical dilemmas. We focused our attention on foetal umbilical cords because we envisioned an autologous application in premature infants who still remain at high risk for pulmonary morbidity and mortality during the first 2 years of life, despite recent improvement in perinatal care. In this regard, the survival of extremely premature newborns has recently increased with the use of new surfactant therapy and antenatal steroids [35]. Inflammatory damage to the airways and distal pulmonary tissue of mechanically ventilated preterm infants might directly affect the alveolar capillary unit and tissue integrity. The alveolus is composed of two epithelial cell types with distinct morphologies. Type-I cells comprise 95% of the alveolar surface and are important for gas exchange, regulation of alveolar fluid levels and stretch-induced modulation of surfactant secretion. Type-II cells are crucial for producing surfactant and regulating alveolar fluid levels and host defence. But notably they are also progenitors for type-I cells during lung development and remodelling, thus the inability

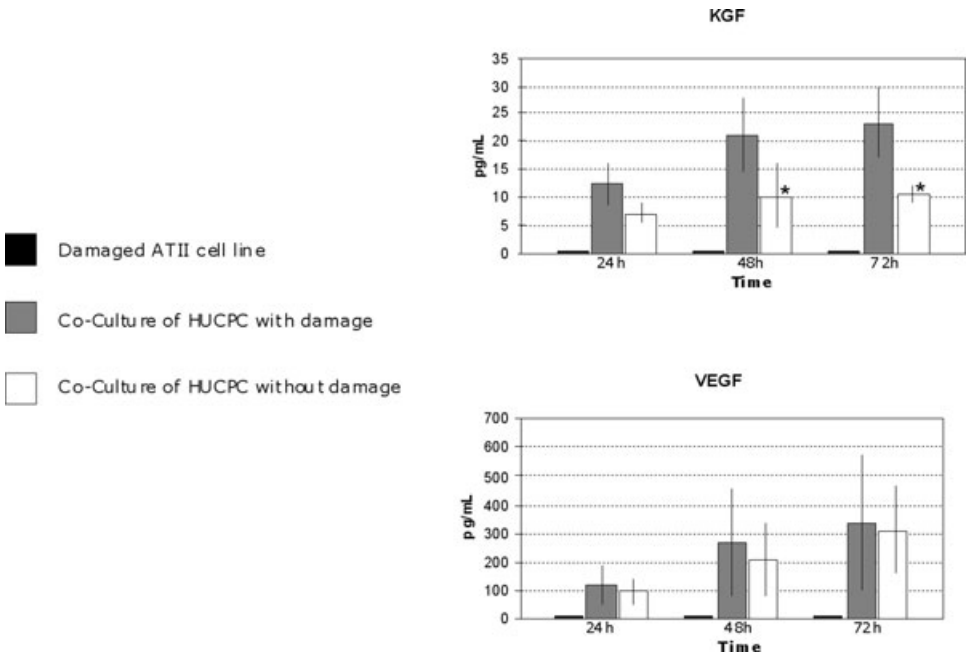

Fig. 7 ELISA assay was used to investigate the presence of soluble factors during the co-culture of foetal PKH26^{+} HUCPC with damaged (grey) rat ATII cell line and without damage (white). In black the soluble factors released by damaged ATII cell line. Supernatants were collected from six independent experiments at different times during the co-culture (24, 48, 72 hrs) and the evaluated soluble factors were KGF, PDGF-BB and VEGF. Data showed an increase of KGF in the co-culture of HUCPC in the presence of the damage (black) in comparison with non damage (grey). KGF was statistically significant at 48 and 72 hrs ($^{*}P < 0.05$). The results are expressed as mean ± S.E.

of type-II cells to proliferate during the first week of life may permanently alter postnatal lung growth during a critical period of postnatal lung development. This disruption in alveolar epithelial cell differentiation might contribute to the pathological processes seen in infants with chronic lung disease or BDP [36]. In this context, we envisioned that HUCPC could represent a novel progenitor for the cell therapy of lung disorders. In the last years, MSC received much attention for their therapeutic potential in various clinical settings of regenerative medicine notwithstanding when tested in animal models of tissue damage they repair the injury and restore the organ function despite the absence of obvious integration and local differentiation in the host damaged tissue. Therefore, other mechanisms should be envisioned to explain these therapeutic results including paracrine effects. In this context and since migration capacity is correlated with *in vivo* homing and represents a predictor for the clinical outcome of cell-treated patients [37], we set up a culture model of tissue damage to document the migration of HUCPC and to evaluate if soluble factors are secreted by them. We observed high levels of KGF and slight modifications in VEGF levels in the co-culture of HUCPC in the presence of damage in comparison with the control cultures, thus indicating that perivascular cells can produce and secrete cytokines that can play beneficial auto- or paracrine roles in tissue repair. Moreover, we observed that conditioned medium containing soluble factors released by the damage has chemotactic potential by itself. In particular, it is noteworthy that KGF plays a critical role in lung development and that it is involved in proliferation, migration, and differentiation of epithelial cells in the skin, cornea, intestines and distal airway [38]. KGF administration has also been shown to protect the lung from a number of toxins (hyperoxia, radiation and bleomycin exposure) [39, 40] and to support the airway epithelium proliferation [41, 42] and differentiation [41]. The secretory profile exhibited by foetal HUCPC in the migration assay shows that *via* paracrine mechanisms they could potentially limit the extension of injury (anti-apoptosis), inhibit scarring and stimulate angiogenesis/vasculogenesis in a clinical setting [43, 44].

In conclusion, given all these findings we demonstrated that HUCPC represent a very promising source of multipotent cells that, in addition to the current therapeutic modalities, could offer an appealing cell-based approach that may have therapeutic effects in various clinical settings including lung disorders.

Acknowledgements

This study was supported by grants from the Italian Ministry of Health (Progetto a Concorso 2008 and 2009, Ex Art. 56), Fondazione Il Sangue, Fondazione NovusSanguis, the Istituto Superiore di Sanità (Malattie Neurodegenerative), the 6FP EU Project – THERCORD and the 7FP EU Project – CASCADE. We thank Dr. Rosaria Giordano for her precious advice. We also thank Gabriella Spaltro and Mariele Viganò for their contribution in molecular studies.

References

1. **Pittenger MF, Mackay AM, Beck SC, *et al.*** Multilineage potential of adult mesenchymal stem cells. *Science.* 1999; 284: 143–7.
2. **Bianco P, Cossu G.** Uno, nessuno e centomila: searching for the identity of mesodermal progenitors. *Exp Cell Res.* 1999; 251: 257–63.
3. **Bianco P, Riminucci M, Gronthos S, *et al.*** Bone marrow stromal stem cells: nature, biology, and potential applications. *Stem Cells.* 2001; 19: 180–92.
4. **Brighton CT, Lorich DG, Kupcha R, *et al.*** The pericyte as a possible osteoblast progenitor cell. *Clin Orthop Relat Res.* 1992; 275: 287–99.
5. **Farrington-Rock C, Crofts NJ, Doherty MJ, *et al.*** Chondrogenic and adipogenic potential of microvascular pericytes. *Circulation.* 2004; 110: 2226–32.
6. **Caplan AI.** All MSCs are pericytes? *Cell Stem Cell.* 2008; 3: 229–30.
7. **Hirschi KK, D'Amore PA.** Pericytes in the microvasculature. *Cardiovasc Res.* 1996; 32: 687–98.
8. **Sims DE.** The pericyte–a review. *Tissue Cell.* 1986; 18: 153–74.
9. **Schwab KE, Gargett CE.** Co-expression of two perivascular cell markers isolates mesenchymal stem-like cells from human endometrium. *Hum Reprod.* 2007; 22: 2903–11.
10. **Dellavalle A, Sampaolesi M, Tonlorenzi R, *et al.*** Pericytes of human skeletal muscle are myogenic precursors distinct from satellite cells. *Nat Cell Biol.* 2007; 9: 255–67.
11. **Zannettino AC, Paton S, Arthur A, *et al.*** Multipotential human adipose-derived stromal stem cells exhibit a perivascular phenotype *in vitro* and *in vivo*. *J Cell Physiol.* 2008; 214: 413–21.
12. **Sarugaser R, Lickorish D, Baksh D, *et al.*** Human umbilical cord perivascular (HUCPV) cells: a source of mesenchymal progenitors. *Stem Cells.* 2005; 23: 220–9.
13. **Crisan M, Yap S, Casteilla L, *et al.*** A perivascular origin for mesenchymal stem cells in multiple human organs. *Cell Stem Cell.* 2008; 3: 301–13.
14. **Ozerdem U, Monosov E, Stallcup WB.** NG2 proteoglycan expression by pericytes in pathological microvasculature. *Microvasc Res.* 2002; 63: 129–34.
15. **Ozerdem U, Grako KA, Dahlin-Huppe K, *et al.*** NG2 proteoglycan is expressed exclusively by mural cells during vascular morphogenesis. *Dev Dyn.* 2001; 222: 218–27.
16. **Li Q, Yu Y, Bischoff J, *et al.*** Differential expression of CD146 in tissues and endothelial cells derived from infantile haemangioma and normal human skin. *J Pathol.* 2003; 201: 296–302.
17. **Middleton J, Americh L, Gayon R, *et al.*** A comparative study of endothelial cell markers expressed in chronically inflamed human tissues: MECA-79, Duffy antigen receptor for chemokines, von Willebrand factor, CD31, CD34, CD105 and CD146. *J Pathol.* 2005; 206: 260–8.
18. **Sacchetti B, Funari A, Michienzi S, *et al.*** Self-renewing osteoprogenitors in bone marrow sinusoids can organize a hematopoietic microenvironment. *Cell.* 2007; 131: 324–36.
19. **Covas DT, Siufi JL, Silva AR, *et al.*** Isolation and culture of umbilical vein mesenchymal stem cells. *Braz J Med Biol Res.* 2003; 36: 1179–83.
20. **Larrivée B, Karsan A.** Isolation and culture of primary endothelial cells. *Methods Mol Biol.* 2005; 290: 315–29.
21. **McElreavey KD, Irvine AI, Ennis KT, *et al.*** Isolation, culture and characterisation of fibroblast-like cells derived from the Wharton's jelly portion of human umbilical cord. *Biochem Soc Trans.* 1991; 19: 29.
22. **Seshareddy K, Troyer D, Weiss ML.** Method to isolate mesenchymal-like cells from Wharton's Jelly of umbilical cord. *Methods Cell Biol.* 2008; 86: 101–19.
23. **Péault B, Rudnicki M, Torrente Y, *et al.*** Stem and progenitor cells in skeletal muscle development, maintenance, and therapy. *Mol Ther.* 2007; 15: 867–77.
24. **Kern S, Eichler H, Stoeve J, *et al.*** Comparative analysis of mesenchymal stem cells from bone marrow, umbilical cord blood, or adipose tissue. *Stem Cells.* 2006; 24: 1294–301.
25. **Kasper M, Barth K.** Bleomycin and its role in inducing apoptotsis and senescence in lung cells-modulating effects of caveolin-1. *Curr Cancer Drug Targets.* 2009; 9: 341–53.
26. **Chen J, Stubbe J.** Bleomycins: towards better therapeutics. *Nat Rev Cancer.* 2005; 5: 102–12.
27. **Aoshiba K, Tsuji T, Nagai A.** Bleomycin induces cellular senescence in alveolar epithelial cells. *Eur Respir J.* 2003; 22: 346–43.
28. **Ennis J, Sarugaser R, Gomez A, *et al.*** Isolation, characterization, and differentiation of human umbilical cord perivascular cells (HUCPVCs). *Methods Cell Biol.* 2008; 86: 121–36.
29. **Stevenson RE, Hall JG.** Human malformations and related anomalies. 2nd ed. New York: Oxford University Press, Inc.; 2006.
30. **Takechi K, Kuwabara Y, Mizuno M.** Ultrastructural and immunohistochemical studies of Wharton's jelly umbilical cord cells. *Placenta.* 1993; 14: 235–45.
31. **Gang EJ, Bosnakovski D, Figueiredo CA, *et al.*** SSEA-4 identifies mesenchymal stem cells from bone marrow. *Blood.* 2007; 109: 1743–51.
32. **Anjos-Afonso F, Bonnet D.** Nonhematopoietic/endothelial SSEA-1+ cells define the most primitive progenitors in the adult murine bone marrow mesenchymal compartment. *Blood.* 2007; 109: 1296–306.
33. **Zangrossi S, Marabese M, Broggini M, *et al.*** Oct-4 expression in adult human differentiated cells challenges its role as a pure stem cell marker. *Stem Cells.* 2007; 25: 1675–80.
34. **Pochampally RR, Smith JR, Ylostalo J, *et al.*** Serum deprivation of human marrow stromal cells (hMSCs) selects for a subpopulation of early progenitor cells with enhanced expression of Oct-4 and other embryonic genes. *Blood.* 2004; 103: 1647–52.
35. **Bland RD**. Neonatal chronic lung disease in the post-surfactant era. *Biol Neonate.* 2005; 88: 181–91.
36. **Speer CP.** Inflammation and bronchopulmonary dysplasia: a continuing story. *Semin Fetal Neonatal Med.* 2006; 11: 354–62.
37. **Vasa M, Fichtlscherer S, Adler K, *et al.*** Increase in circulating endothelial progenitor cells by statin therapy in patients with stable coronary artery disease. *Circulation.* 2001; 103: 2885–90.
38. **Barazzone C, Donati YR, Rochat AF, *et al.*** Keratinocyte growth factor protects alveolar epithelium and endothelium from oxygen-induced injury in mice. *Am J Pathol.* 1999; 154: 1479–87.
39. **Panos RJ, Bak PM, Simonet WS, *et al.*** Intratracheal instillation of keratinocyte growth factor decreases hyperoxia-induced mortality in rats. *J Clin Invest.* 1995; 96: 2026–33.

40. **Deterding RR, Havill AM, Yano T, *et al.*** Prevention of bleomycin-induced lung injury in rats by keratinocyte growth factor. *Proc Assoc Am Physicians.* 1997; 109: 254–68.
41. **Yano T, Mason RJ, Pan T, *et al.*** KGF regulates pulmonary epithelial proliferation and surfactant protein gene expression in adult rat lung. *Am J Physiol Lung Cell Mol Physiol.* 2000; 279: 1146–58.
42. **Portnoy J, Curran-Everett D, Mason RJ.** Keratinocyte growth factor stimulates alveolar type II cell proliferation through the extracellular signal-regulated kinase and phosphatidylinositol 3-OH kinase pathways. *Am J Respir Cell Mol Biol.* 2004; 30: 901–7.
43. **Kinnaird T, Stabile E, Burnett MS, *et al.*** Local delivery of marrow-derived stromal cells augments collateral perfusion through paracrine mechanisms. *Circulation.* 2004; 109: 1543–9.
44. **Tang YL, Zhao Q, Qin X, *et al.*** Paracrine action enhances the effects of autologous mesenchymal stem cell transplantation on vascular regeneration in rat model of myocardial infarction. *Ann Thorac Surg.* 2005; 80: 229–37.